J. Electrochem. Sci. Eng. **15(5)** (2025) 2729; http://dx.doi.org/10.5599/jese.2729

Open Access : : ISSN 1847-9286
www.jESE-online.org

Original scientific paper

Ion-imprinted polyaniline-based polymer for selective electrochemical detection of cadmium

Eldhose V. Varghese[1], Roshny Roy[1], Carsten Schwandt[2], Praveen C. Ramamurthy[3] and Alex Joseph[1,✉]

[1]*Department of Chemistry, Newman College, Thodupuzha, 685585, India*
[2]*Advanced Materials Center & Faculty of Electronics, Telecommunications and Informatics, Gdańsk University of Technology, Gdańsk, Poland*
[3]*Department of Materials Engineering, Indian Institute of Science, Bangalore, 560012, India*

Corresponding author: ✉alex.joseph@newmancollege.ac.in

Received: March 24, 2025; Accepted: May 24, 2025; Published: June 29, 2025

Abstract

An electrochemical sensor based on ion-imprinted functionalized polyaniline has been fabricated and tested for the electrochemical sensing of cadmium in aqueous solution. The synthesis of the polymer was started by copolymerizing anthranilic acid and 2-(1H-benzimidazol-2-yl) aniline in the presence of Cd^{2+} ions as the target analyte and followed by acid leaching out the analyte to obtain the ion-imprinted polymer (IIP). The synthesized IIP was examined for its structural, crystallographic and morphological characteristics using Fourier-transform infrared spectroscopy, X-ray diffraction analysis and field-emission scanning electron microscopy. The IIP has been used to modify a carbon paste electrode (CPE), and the IIP-modified CPE was tested for the sensitive and selective detection of Cd^{2+} ions in aqueous solution. The key electrode preparation parameters, i.e. Cd deposition potential, pH of deposition solution, deposition time, and thickness of active layer, were optimized using pulse voltammetric stripping analysis to achieve maximum performance. Electrochemical investigations with the optimized IIP-modified CPE revealed a high sensitivity for Cd^{2+} ions as well as a high selectivity in the presence of potentially interfering ions. Reproducibility and repeatability of the electrode were assessed and found to be satisfactory.

Keywords

Functionalization; ion-imprinted polymer; electrochemical sensor; selectivity

Introduction

Cadmium is a non-essential toxic element present naturally in trace levels in the environment. Major occupational sources of cadmium pollution are the ore mining and metallurgical industries, as well as the production of pigments, plastic stabilizers and nickel-cadmium batteries [1,2], while environmental sources are the emissions from volcanoes and the weathering of erupted pyroclasts

and ashes [3]. Cadmium exposure mainly occurs through ingestion of contaminated water and food, inhalation of polluted air, and smoking cigarettes [1,2]. Through anthropogenic introduction and biomagnification in the human body, cadmium can cause many deleterious effects, including renal tubular dysfunction, glucose metabolism disorders, osteomalacia, osteoporosis, as well as lung, pancreatic and breast cancer, cardiac failure and cerebral infarction [4-6]. Metalloregulatory mechanisms based on metallothioneins control metal ion homeostasis and detoxification of cells in the human body, but these fail above a tolerance limit [7]. Consequent to its high mobility, tendency for bioaccumulation and long half-life, cadmium also affects enzymes and soil colloids and thereby induces adverse effects on plants, including reduced respiration and photosynthesis, increased oxidative stress and leaf chlorosis, as well as inhibited nutrient uptake and growth [8-11].

The International Agency for Research on Cancer (IARC) categorized cadmium as a Group 1A carcinogenic element [12], and the World Health Organization (WHO) ascertained the permissible cadmium ion concentration in drinking water as 3 ng mL^{-1} [13]. Owing to its high toxicity even in low concentrations, the accurate determination of cadmium in water is imperative. The prevailing conventional analytical methods are inductively coupled plasma atomic emission spectrometry (ICP-AES) [14], graphite furnace atomic absorption spectrometry (GFAAS) [15], and flame atomic absorption spectrometry (FAAS) [16]. Optical biosensors [17,18] are also considered for analysis of both water and dietary samples. Electrochemical techniques like cyclic voltammetry (CV), chronoamperometry (CA), and especially differential pulse anodic stripping voltammetry (DPASV) [19] are regarded as possible low-cost alternatives, as they have the potential to offer highly sensitive, easy-to-use and portable instruments that can be adapted for onsite measurements. For recent reviews on sensing materials and techniques for the detection of cadmium, as well as possible restoration strategies using adsorption on nanostructured carbon-based materials and microbial bioremediation, the reader is referred to the literature [8,20,21].

Molecularly-imprinted polymers (MIP) are materials with specific molecular recognition sites that bind to a particular analyte, thus markedly enhancing their interaction with this analyte in solution. MIP technology is hence an effective way to improve the sensitivity and selectivity in electrochemical sensing [22,23]. Tchekwagep *et al.* [24] have reviewed the use of MIPs for the selective detection of inorganic species, and Ramanavicius *et al*. have covered the use of conducting polymers for MIPs [25] and their application in the biomedical and pharmaceutical sectors [26]. In the same manner, ion-imprinted polymers (IIP) can be used for the sensing of specific ions. Several studies on Cd^{2+} ion sensing through IIPs in combination with electroanalytical methods have already been reported in the literature. With regard to the sensing material, use has been made of specific chelators entrapped in a polymeric matrix [27,28], copolymers based on 4-vinyl pyridine [29-32] or methacrylate and methacrylic acid [28,32-37], conducting polymers based on pyrrole [38] or o-phenylenediamine [39,40], as well as composite materials such as chitosan with gold nanoparticles and graphene [41], chitosan with N-doped graphene oxide [42], and reduced graphene oxide decorated with TiO_2 nanoparticles [43]. With respect to specific electrode designs, efforts have covered screen-printed electrodes using electropolymerized 4-aminophenylacetic acid [44], and interdigitated electrodes using an ethylenimine/methacrylic acid copolymer functioning as a chemical resistor [45].

Polyaniline should be particularly advantageous for the synthesis of IIP matrices because it possesses a high intrinsic conductivity and relatively facile chemical functionalizability of the polymer backbone [46] and, moreover, because its nanostructured form enables enhanced sensitivity as a result of the very high specific surface area [47]. Presnyakov *et al.* [48] have recently provided an

overview highlighting the scope of polyaniline in imprinted polymer applications, and several reports confirm that it is indeed suitable for the selective sensing of inorganic [49], organic [50,51], and biochemical [52,53] analytes. Beyond that, polyaniline is a cost-affordable choice of material for large-scale manufacture, especially when compared with the various nanostructured composites.

Related earlier work from our group has focused on the straightforward functionalization of polyaniline with imidazole [54,55] for the sensitive electrochemical detection of heavy metal ions. Following on from these efforts, we have herein synthesized the first polyaniline-derived IIP for the detection of Cd^{2+} ions. The IIP contains a benzimidazole group and a carboxylic acid group in its backbone, which together serve as a metal-coordinating site for the highly sensitive and selective electrochemical detection of Cd^{2+} ions. The synthesis was carried out by, firstly, copolymerizing in-situ the monomers of 2-aminobenzoic acid, commonly known as anthranilic acid, and 2-(1H-benzimidazol-2-yl) aniline in the presence of Cd^{2+} ions as the target analyte and, secondly, leaching out the target analyte to leave behind a nanostructured polyaniline matrix with ion-imprinted cavities that are specific to Cd^{2+} ions. The resultant IIP has been used as the active material for the modification of a carbon paste electrode (CPE) and then trialled for the electrochemical detection of Cd^{2+} ions in aqueous media. The electroanalytical techniques applied were cyclic voltammetry (CV) and differential pulse anodic stripping voltammetry (DPASV), and the electrode was evaluated in view of sensitivity, selectivity, reproducibility and repeatability.

Experimental

Materials and methods

All the chemicals used for synthesis were of analytical grade and used without further purification unless otherwise mentioned. 2-aminobenzoic acid (anthranilic acid) was acquired from Loba Chemie Pvt. Ltd., India and recrystallized from methanol before use, while 2-(1H-benzimidazol-2-yl) aniline was acquired from AstaTech Inc., USA. Ammonium peroxodisulfate (APS) and concentrated hydrochloric acid were obtained from Nice Chemicals Pvt. Ltd., India, and cadmium nitrate tetrahydrate was obtained from Merck India Pvt. Ltd., India. Graphite powder was received from Sigma Aldrich Chemicals Pvt. Ltd., India. The salts and acids containing the ions used in the selectivity studies, LiCl, NaCl, KCl, $MgCl_2$, $CaCl_2$, $BaCl_2$, $Pb(NO_3)_2$, $MnCl_2$, $FeCl_2$, $CoCl_2$, $ZnCl_2$, $CdCl_2$, $Hg(NO_3)_2$, NH_4Cl, HNO_3, HCl and H_2SO_4, were acquired from S D Fine Chem Ltd., India. Rectified ethanol was obtained from Kerala Excise Department, Government of Kerala, India. Deionized (DI) water was used throughout the experimental protocols.

The chemical structure of the polymers synthesized was analysed by Fourier-transform infrared spectroscopy (FTIR) using a Thermo Scientific Nicolet i5 spectrometer with an ATR module. The crystalline nature of the polymers was examined by X-ray diffractometry (XRD) using a Rigaku MiniFlex 600 diffractometer at a scan rate of 5° min^{-1}. Their surface morphology was investigated by field-emission scanning electron microscopy (FESEM) using a JEOL JSM-6490LA microscope. All electrochemical studies were performed with a Metrohm Autolab PGSTAT302N workstation. A three-electrode configuration was used, comprising an in-house-made CPE of 4 mm diameter as the working electrode, a saturated calomel electrode (SCE) from CH Instruments, USA as the reference electrode, and a platinum wire as the counter electrode.

Synthesis of ion-imprinted polymer

2.74 g of anthranilic acid (0.02 moles) was dissolved in 30 mL of 1:1 ethanol-water solution and stirred magnetically for 5 min. Added to this were 4.18 g of 2-(1H-benzimidazol-2-yl) aniline

(1.0 equivalent, 0.02 moles) and 6.16 g of $Cd(NO_3)_2{\cdot}4H_2O$ (1.0 equivalent, 0.02 moles) in 30 mL of 1:1 ethanol-water. The mixture was heated to 70 °C for 6 h with constant stirring to ensure complete metal complexation. The resultant solution was then treated with 5.01 g of ammonium peroxodisulfate (1.1 equivalent, 0.022 moles) in 20 mL of 0.1 M HCl to initiate the polymerization and left for 24 h to complete the reaction. The resultant polymer was washed, dried in a vacuum oven at 60 °C, and triturated. This polymer, incorporating bonded Cd^{2+} ions, is designated as Cd-IIP. Next, the Cd-IIP was subjected to Soxhlet extraction using 0.1 M HNO_3 for 24 h to completely remove the Cd^{2+} ions from the polymer. The resultant material was washed with DI water until neutral and dried in a vacuum oven at 60 °C to obtain the ion-imprinted polymer, denoted as IIP. A similar synthesis procedure was carried out without adding Cd^{2+} ions to get the analogous non-imprinted polymer, denoted as NIP. This was used as a reference material in various parts of the study.

Preparation of IIP-modified carbon paste electrode

Carbon paste was prepared by blending graphite powder and paraffin oil in a 7:3 mass ratio for 72 h in a ceramic ball mill. The carbon paste was then filled into a glass tube of 4 mm inner diameter to a length of 8 mm, enclosing a silver wire as an electric contact. The resultant carbon paste electrode (CPE) surface was polished on a smooth paper sheet before use.

A dispersion of each polymer used for modification of the CPE, *i.e.* IIP and NIP, was prepared by adding 1 mg of the respective polymer to 1 mL of DI water, stirring overnight, and sonicating for 1 h. The dispersion was then drop-coated onto the CPE surfaces and allowed to dry overnight in order to obtain the respective modified electrodes, *i.e.* CPE-IIP and CPE-NIP.

Results and discussion

Synthetic route

A schematic representation of the synthesis of Cd-IIP and IIP is displayed in Scheme 1. In the first step, Cd-IIP was synthesized from the precursors, anthranilic acid and 2-(1H-benzimidazol-2-yl) aniline, in ethanol-water in the presence of $Cd(NO_3)_2{\cdot}4H_2O$, using thin-layer chromatography (TLC) to check completion of the reaction.

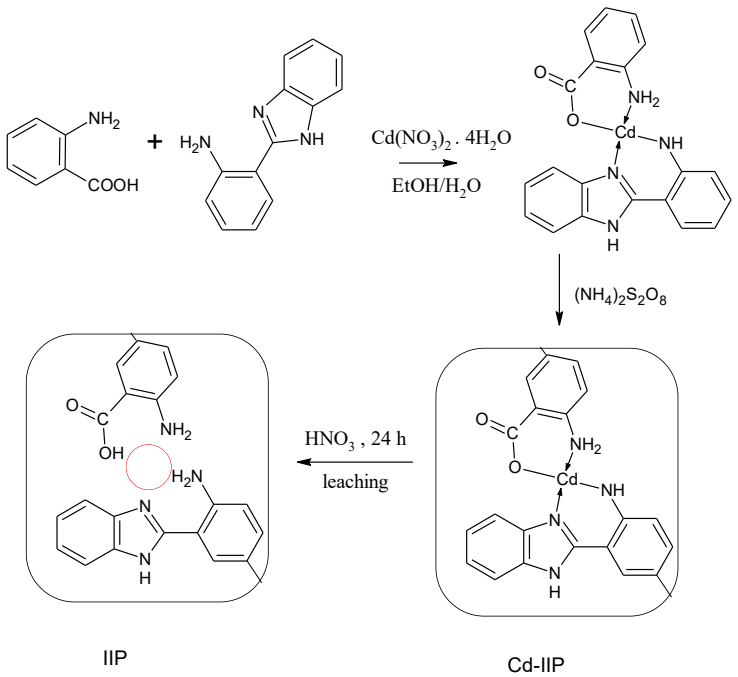

Scheme 1. *Schematic representation of synthesis of Cd-IIP and IIP*

In the second step, the cadmium complex formed was subjected to polymerization, using ammonium peroxodisulfate as an oxidizing agent that links the aniline moieties. In the final step, IIP was formed by acid leaching the coordinated Cd^{2+} ions, to yield a polymeric matrix that possesses cavities that exactly match the size of the Cd^{2+} ion.

Materials characterization

The chemical structures of the polymers were characterized by FTIR, and the spectra recorded are presented in Figure 1. As expected, the spectra exhibit characteristic peaks that correspond to the polyaniline backbone and the functional groups.

In the case of NIP, the absorption peaks and bands can readily be assigned to structural features based on information from the literature [56-60]. The peaks at 1569 and 1496 cm^{-1} originate from the stretching vibrations in the quinoid and benzenoid rings of the polymer backbone, respectively. The peak at 1698 cm^{-1} is associated with the C=O stretching vibration of the carboxyl group on the polymer backbone, and the peak at 1238 cm^{-1} stems from the stretching vibrations in the benzimidazole ring. The broad band around 3222 cm^{-1} is associated with the N-H/O-H stretching vibrations of the polymer backbone, and the broad band around 2915 cm^{-1} stems from the C-H stretching vibration of the aromatic rings. The peak appearing at 1133 cm^{-1} is due to the C-H in-plane bending vibration of the benzimidazole ring, and the peak at 755 cm^{-1} is due to the C-H out-of-plane bending vibration of the benzene ring.

For Cd-IIP, the peaks and bands observed are similar to those for NIP, thus pointing to the presence of the same structural features in the polyaniline backbone and the functional groups. Notably, the peak from the C=O stretching vibration of the carboxyl group is shifted from 1698 cm^{-1} in NIP to 1680 cm^{-1} in Cd-IIP, and the band from the N-H/O-H stretching vibrations is shifted from 3222 cm^{-1} in NIP to 3206 cm^{-1} in Cd-IIP. These changes corroborate that the coordination of the Cd^{2+} ions in Cd-IIP occurs through both the oxygen of the carboxyl group and the nitrogen of the amino group.

For IIP, *i.e.* after removal of the Cd^{2+} ions from Cd-IIP, the same features are again observed. The shifts of the main peak positions from Cd-IIP to IIP are all minor, *i.e.* from 742, 1124, 1245, 1499, 1600 and 1680 cm^{-1} in Cd-IIP to, respectively, 746, 1133, 1232, 1504, 1573 and 1690 cm^{-1} in IIP. These changes are indicative of the relief of steric effects when the Cd^{2+} ion is taken out of the structure.

In conclusion, the similarities of the FTIR spectra of NIP, Cd-IIP and IIP prove that neither the presence of the Cd^{2+} ions during polymerization nor their removal after polymerization has altered the chemical structure of the polymer.

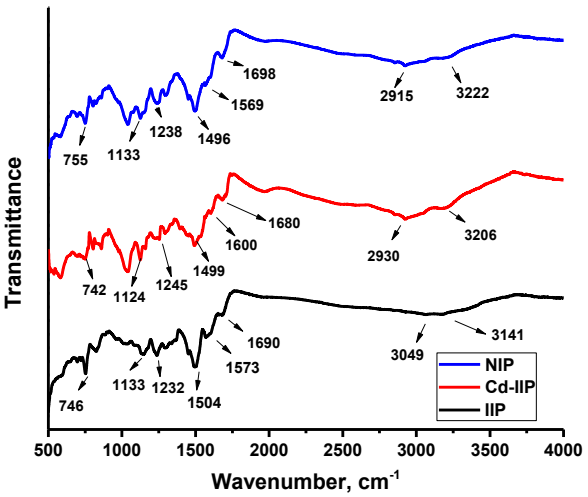

Figure 1. *Fourier-transform infrared spectra of NIP, Cd-IIP and IIP*

The crystallographic properties of the polymers were evaluated by XRD, and the diffractograms recorded are compiled in Figure 2. The diffractogram of NIP exhibits several characteristic peaks between 5 and 30° that indicate a significant level of crystallinity. The peaks at 20.2 and 26.6° may be attributed to the periodic repetition of the benzenoid and quinoid rings in adjacent polymer chains [61,62], while the peaks at 9.2 and 12.9° may be ascribed to the periodic arrangement of nitrogen and dopant atoms [62]. The dopant in the given case is chloride ions, whose presence arises from the use of HCl in the synthesis protocol. The peak positions of 9.2, 12.9, 16.0, 20.2 and 26.6° correspond to *d*-spacings of 0.96, 0.69, 0.55, 0.44 and 0.34 nm, respectively, which are similar to those reported for the emeraldine salt of polyaniline [63]. In the diffractogram of Cd-IIP, the peaks are shifted to slightly larger *d*-spacings compared with NIP, indicating that the Cd-IIP matrix has expanded somewhat due to the incorporation of Cd^{2+} ions. The diffractogram of IIP, recorded after removal of the Cd^{2+} ions, is practically identical with that of NIP. Altogether, the XRD analysis has shown that the three polymers have the same crystal structure and similar *d*-spacings.

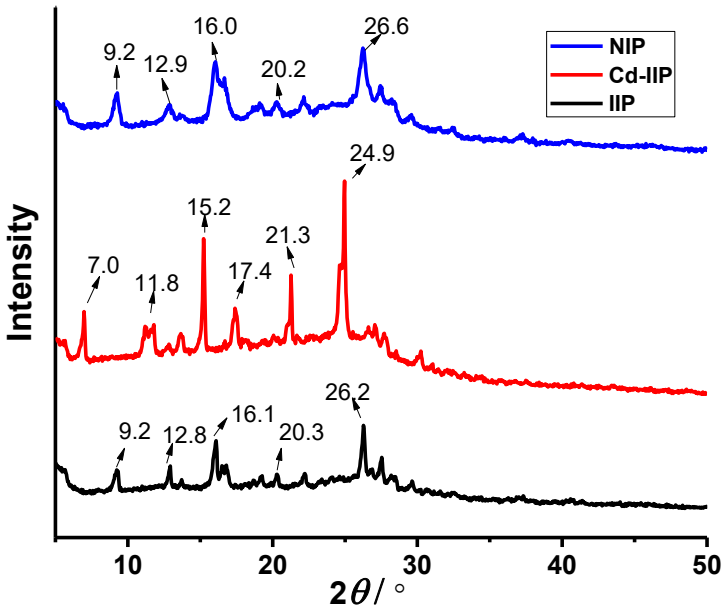

Figure 2. *X-ray diffractograms of NIP, Cd-IIP and IIP*

The surface morphologies of the polymers were assessed by FESEM, and the micrographs taken are collected in Figure 3. It is observed that NIP, Cd-IIP and IIP all have an agglomerated nanosphere structure. The formation of these nanospheres has been explained based on micelle formation of the monomers prior to the chemical polymerization reaction [64]. The average diameters of the agglomerates in NIP, Cd-IIP and IIP are measured to be 23±2, 39±2.5 and 31±3.7 nm, respectively. The larger agglomerate size in Cd-IIP compared with that of NIP indicates that the presence of the Cd^{2+} ions may have facilitated the agglomeration of the monomers before polymerization. Notably, IIP has a similar nanostructure to Cd-IIP. While the agglomerate size in IIP has diminished slightly, it is evident that the acid leaching process has not changed the nanostructure to a substantial extent. Overall, the SEM analysis has shown that the polymers possess extremely large specific surfaces, which is highly beneficial as it will enhance the accumulation of target ions in solution and hence improve sensitivity in electrochemical sensing applications.

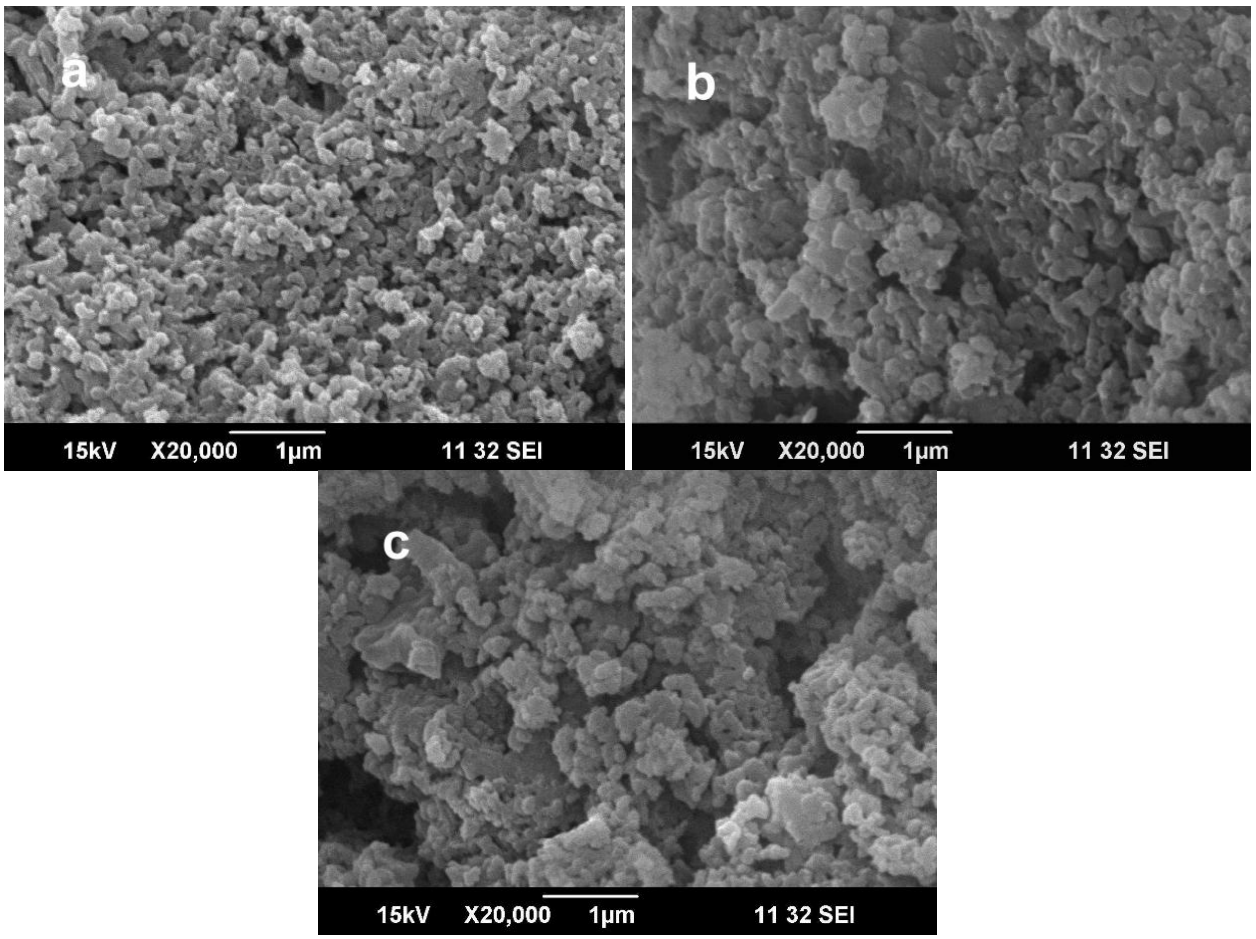

Figure 3. *Scanning electron microscopic images of (a) NIP, (b) Cd-IIP and (c) IIP*

Cyclic voltammetry studies

The abilities of the bare and modified CPEs for the sensing of Cd^{2+} ions were assessed in CV studies, and the voltammograms recorded are presented in Figure 4. The experimental conditions were an acetate buffer solution of pH 5.0 and a potential range from +0.5 to -1.8 V *vs.* SCE at a scan rate of 50 mV s^{-1}.

The bare CPE in the plain buffer solution shows no features on its CV (black solid line). This indicates that it serves as an inert sensor substrate. Both the CPE-NIP and CPE-IIP exhibit small features on their CVs in the plain buffer solution (blue and red solid lines). These represent a redox couple at around -0.8 and -0.7 V that originates from, respectively, reduction and oxidation reactions of the functionalized polyaniline, as reported in the literature before [65].

In contrast, in the presence of Cd^{2+} ions in the buffer solution, the bare CPE, CPE-NIP and CPE-IIP all display additional and more pronounced features (black, blue and red dashed lines). These represent a redox couple at around -1.2 and -0.9 V that is ascribed to, respectively, the reduction of Cd^{2+} ions to Cd metal and the oxidation of Cd metal back to Cd^{2+} ions. The peaks related to Cd are in distinctly different positions from the peaks from the functionalized polyaniline and can, therefore, be used unambiguously for analytical purposes. The peak currents are highest for CPE-IIP, followed by CPE-NIP and bare CPE, demonstrating the superior ion-coordinating ability of IIP. This observation is attributed to the existence of the specially-designed ion-imprinted cavities in the polymer.

Altogether, the CV results have suggested that CPE-IIP has good electrocatalytic activity towards Cd^{2+} ions in aqueous solution that can be exploited for electrochemical sensing.

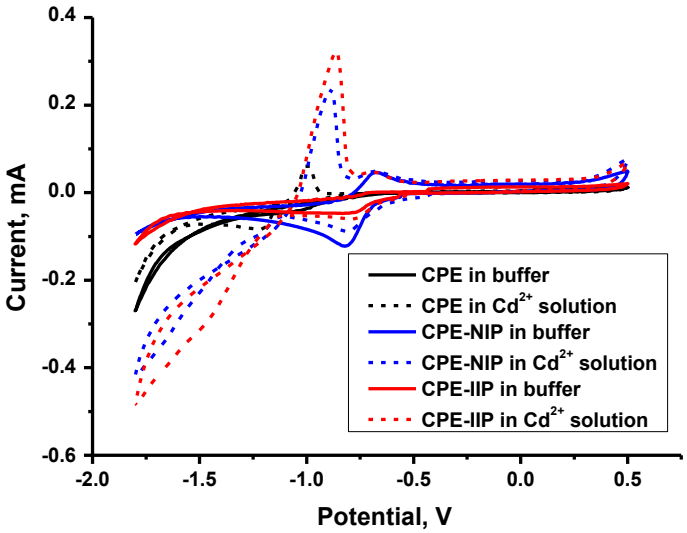

Figure 4. *Cyclic voltammograms of bare CPE, CPE-NIP and CPE-IIP recorded in acetate buffer solution of pH 5.0 in the absence and presence of Cd^{2+} ions; the concentration of Cd^{2+} ions is 0.1 mM when present*

Differential pulse anodic stripping voltammetry studies

Following on from the CV results, the ability of CPE-IIP to sense Cd^{2+} ions was evaluated further by DPASV studies and compared with CPE-NIP as the reference material. Each individual experiment involved two steps: firstly, pre-concentrating Cd onto the CPE surface by applying a suitable deposition potential and, secondly, stripping the Cd off the CPE surface by reversing the potential. Mechanistically, in the pre-concentration step, Cd^{2+} ions from the solution are deposited onto the electrode surface and reduced to Cd metal, Equation (1):

$$Cd^{2+} \rightarrow Cd_{deposited} \quad (1)$$

In the stripping step, the Cd metal is reoxidized to Cd^{2+} ions that dissolve back into solution, Equation (2):

$$Cd_{deposited} \rightarrow Cd^{2+} \quad (2)$$

Efforts were undertaken to optimize the electrode parameters, namely, Cd deposition potential, pH of deposition solution, deposition time, and thickness of the active IIP layer on the electrode surface. In these experiments, 10 mL of an aqueous acetate buffer was used, and the anodic sweeping step was carried out by changing the potential from -0.8 to 0 V *vs.* SCE at a scan rate of 50 mV s^{-1} and the stripping current was recorded.

The Cd deposition potential and the pH of deposition solution are mutually correlated factors that strongly influence the Cd anodic stripping current. Therefore, both quantities were optimized together by randomly selecting deposition potentials between -1.0 and -1.5 V *vs.* SCE and pH values of the acetate buffer between 3.5 and 5.5. A total of 15 experiments were conducted with different sets of values to establish the correlation diagram. The anodic stripping current as a function of both the deposition potential and the pH is displayed in Figure 5. It is observed that, as the deposition potential is increased from -1.0 to -1.2 V, the stripping current increases substantially, whereas any further increase of the potential leads to a decrease in the current. Similarly, as the pH is increased from 3.5 to 5.0, the stripping current increases, while a further rise in pH causes a current decline. This is probably because the degree of protonation of the water molecules around the Cd^{2+} ions diminishes. The results show that the optimal pre-concentration of Cd on the electrode surface is accomplished for a deposition potential of -1.2 V and a pH of 5.0, so these values were selected for further DPASV analysis.

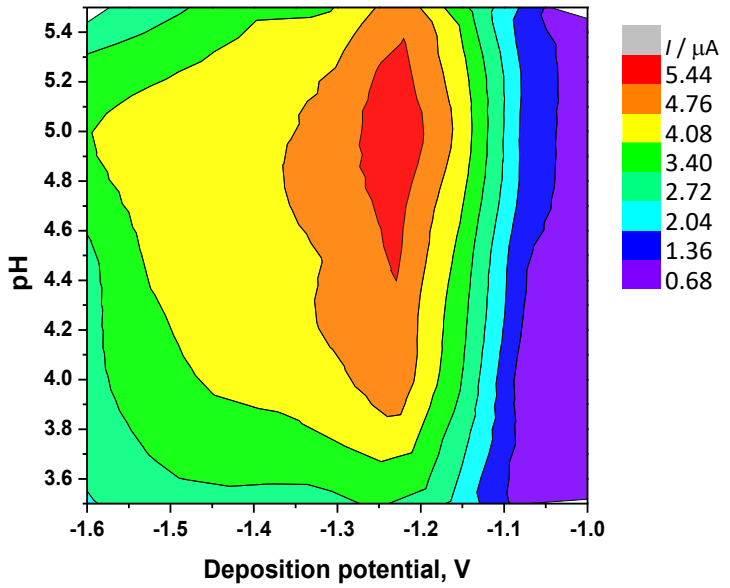

Figure 5. *Combined effect of Cd deposition potential vs. SCE and pH of deposition solution on the anodic stripping current*

The influence of the deposition time on the anodic stripping current was also investigated, with the results shown in Figure 6a. It is seen that the stripping current increases as the deposition time increases, reaching a maximum after about 15 min, whereas further increasing the time does not alter the current significantly. This is likely due to the saturation of active binding sites on the electrode surface. Finally, the effect of the thickness of the active IIP layer coated onto the CPE surface was examined, as shown in Figure 6b. Experimentally, this was done by using different volumes of deposition solution and assuming that these scale directly with the layer thickness attained on the electrode surface. It is seen that the stripping current increases as the volume of deposition solution increases to about 25 µL, and then falls. This is because while the growing layer offers an increasing number of binding sites, it finally becomes too resistive to facilitate charge transfer. Based on these results, a deposition time of 15 min and an active layer thickness corresponding to a volume of deposition solution of 25 µL were chosen in the further studies.

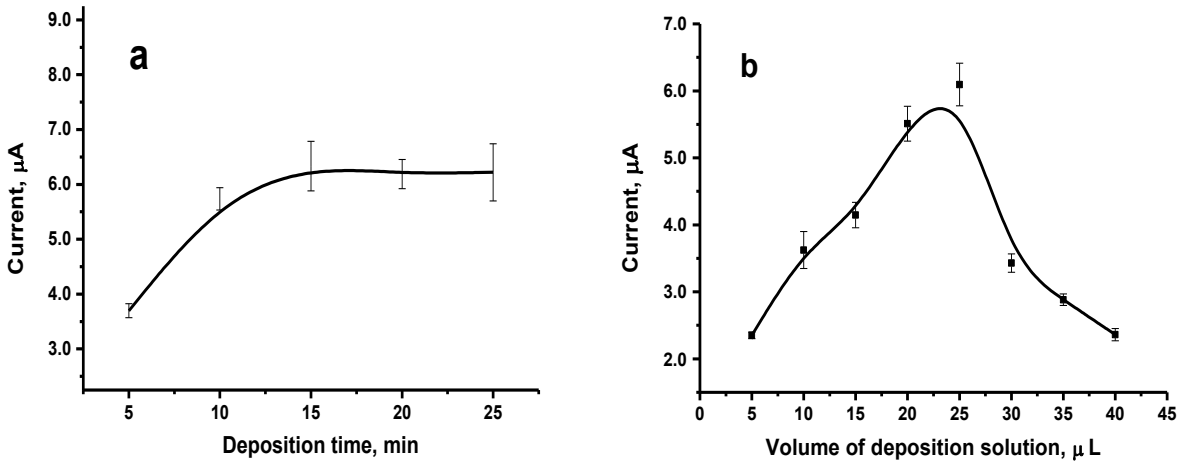

Figure 6. *Effect of (a) deposition time and (b) volume of deposition solution (scaling with active layer thickness) on the anodic stripping current*

Calibration plot and limit of detection

In order to determine the limit of detection (LOD) of the proposed sensor, CPE-IIP and CPE-NIP were investigated by DPASV in Cd^{2+} ion solutions with concentrations ranging from 1 to 10000 nM. The experimental conditions followed were as previously optimized: deposition potential of -1.2 V *vs.* SCE, 10 mL of acetate buffer of pH 5.0, deposition time of 15 min, and active layer thickness corresponding to 25 µL of deposition solution added. The other instrumental parameters were: 50 mV s^{-1} scan rate, 100 mV pulse amplitude, and 40 ms pulse period.

The calibration plots for CPE-IIP and CPE-NIP were obtained by measuring the anodic stripping currents as a function of Cd^{2+} ion concentration. The calibration plots for both are presented in Figures 7a and 7b. It is seen that in both cases the anodic stripping current increases with the analyte concentration and that there are two linear regimes, and the currents for CPE-IIP are higher than those for CPE-NIP. In the case of CPE-IIP, the first linear region is found between the concentrations of 1 and 800 nM with an R^2 value of 0.9986 (line AB) and the second region is between 0.8 and 10 µM with an R^2 value of 0.9989 (line BC). In these regions, CPE-IIP may be utilized for the determination of Cd^{2+} ions with a high degree of accuracy. Similarly, in the case of CPE-NIP, the first linear region is found for concentrations from 50 and 700 nM with an R^2 value of 0.9979 (line AB) and the second linear region is from 700 to 10000 nM with an R^2 value of 0.9962 (line BC).

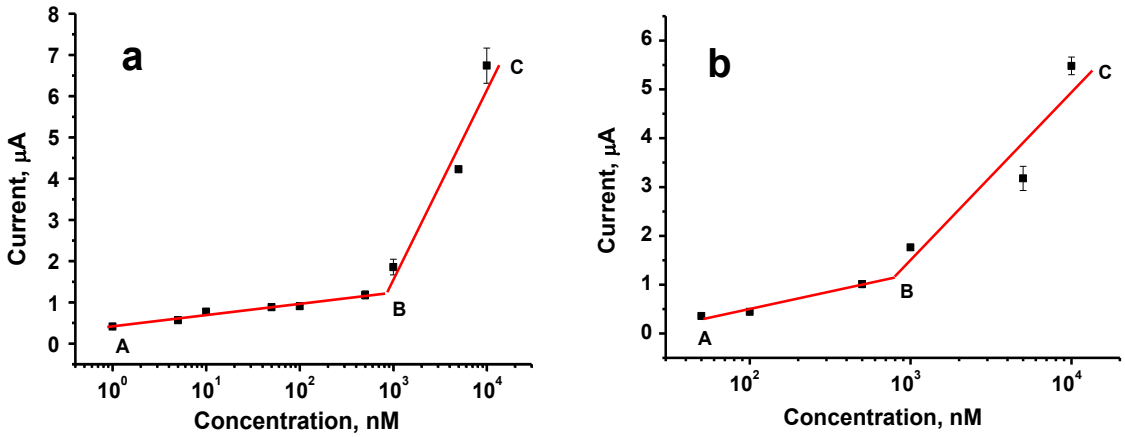

Figure 7. *DPASV calibration plots for Cd^{2+} ion concentrations of (a) CPE-IIP and (b) CPE-NIP in acetate buffer solution of pH 5.0*

The LOD of the sensor is calculated using the equation LOD = $3S_a/b$, where S_a is the standard deviation of the lowest concentration measured, and b is the slope of the regression line. In the case of CPE-IIP, the LOD of the low-concentration line is 0.506 nM, while for CPE-NIP it is 15.6 nM. CPE-IIP thus possesses a superior sensitivity compared with CPE-NIP.

A comparison of the IIPs tested for Cd^{2+} ion sensing reported in the literature with the one developed in the current work is provided in Table 1. It is seen that the sensor described here compares favourably with the others, exhibiting linearity over more than four orders of magnitude and a LOD at the lower end.

Table 1. *Characteristics of ion-imprinted sensors for cadmium detection*

Modified electrode	Analysis method	Linear range, nmol L^{-1}	LOD, nmol L^{-1}	Ref.
IIP/CPE	DPASV	4.4 to 360	1.30	[27]
IIP/CPE	DPASV	4.0 to 500	1.94	[28]
IIP/CPE	ASV	1.0 to 500	0.52	[29]
IIP-SiO_2/MWCNT-CPE	POT	100 to 10^7	100	[30]

Modified electrode	Analysis method	Linear range, nmol L^{-1}	LOD, nmol L^{-1}	Ref.
IIP/Fe_3O_4-SiO_2-GCE	DPV	8.0 to 50 and 50 to 800	0.10	[31]
IIP/CPE	DPV	90 to 24,000; 24,000 to 60,000 and 60,000 to 170,000	44.0	[32]
IIP/CPE	DPASV	18 to 1800	2.80	[33]
IIP/GDE	POT	200 to 10^7	100	[34]
IIP/MWCNT-Pt	CV	8900 to 44,000	30	[35]
IIP/GO-GCE	ASV	0.0042 to 5.6×10^6	7.0×10^{-5}	[36]
IIP/CPE	DPV	1.0 to 10^5	0.143	[37]
IIP/rGO-GCE	SWASV	8.9 to 890	2.3	[38]
IIP/rGO-GCE	SWASV	8.9 to 440	1.2	[39]
IIP/rGO-GCE	SWASV	8.9 to 890	0.98	[40]
IIP-Au-rGO/GCE	DPV	100 to 900	0.162	[41]
IIP/N-rGO-GCE	DPV	10 to 100	3.51	[42]
IIP-SiO_2/rGO-TiO_2-GCE	DPV	10 to 10,000	12	[43]
IIP film/SPCE	CV	10 to 1200	1.71	[44]
IIP/rGO-CR	Chemiresistor	18 to 1800	7.4	[45]
IIP/CPE	DPASV	1.0 to 800 and 800 to 10,000	0.506	This work

CPE: carbon paste electrode, GCE: glassy carbon electrode, GDE: graphite disk electrode, GO: graphene oxide, rGO: reduced graphene oxide, N-rGO: nitrogen-doped reduced graphene oxide, SPCE: screen-printed carbon electrode, CR: chemiresistor; DPASV: differential pulse anodic stripping voltammetry, ASV: anodic stripping voltammetry, POT: potentiometry, DPV: differential pulse voltammetry, CV: cyclic voltammetry, SWASV: square wave anodic stripping voltammetry.

Selectivity towards Cd^{2+} ions

Selectivity of a sensor, *i.e.* the ability to detect the analyte in the presence of other species, is a parameter of paramount importance in any sensing application. The selectivity of CPE-IIP towards Cd^{2+} ions was determined by DPASV, recording the anodic stripping currents in aqueous solutions containing Cd^{2+} ions together with potentially interfering ions, such as alkali metal, alkaline earth metal, heavy metal and transition metal cations, as well as some common anions. Figure 8a compiles the anodic stripping currents obtained for solutions containing 1 μM of Cd^{2+} ions in addition to 100 equivalents of Li^+, Na^+, K^+, Mg^{2+}, Ca^{2+}, Ba^{2+}, Pb^{2+}, Mn^{2+}, Fe^{2+}, Co^{2+}, Zn^{2+}, Hg^{2+}, NH_4^+, NO_3^-, Cl^-, and SO_4^{2-}. The results signify that CPE-IIP is highly selective for Cd^{2+} ions in the presence of the above ions, even if those occur at a considerably higher concentration than the Cd^{2+}. The observations hence indicate that the void created in the polymeric structure after leaching out the Cd^{2+} ion does indeed stay structurally stable and thereby provides a perfect fit for this ion in the given sensing application.

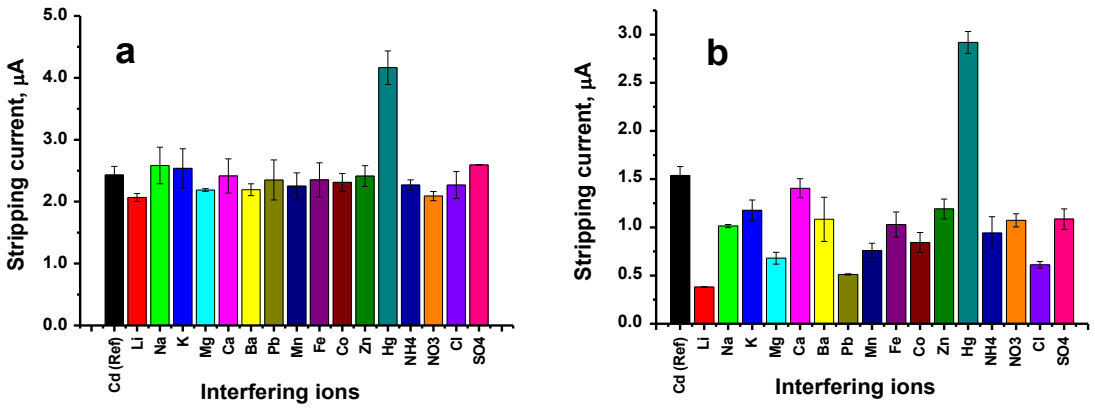

Figure 8. *Selectivity of (a) CPE-IIP and (b) CPE-NIP in acetate buffer containing 1 μM Cd^{2+} ions and 100 equivalents of the potentially interfering ions*

The only exception is Hg^{2+}, likely due to its ability to facilitate the co-deposition with Cd^{2+} and thus the formation of Cd-Hg amalgam [66]. For comparison, Figure 8b shows the corresponding results for CPE-NIP. In stark contrast to CPE-IIP, CPE-NIP is much more strongly affected by almost all of the ions tested.

Stability and reusability

The long-term stability and multiple reusability of a sensor are further critical parameters. The stability of CPE-IIP over time was assessed by first preparing a set of individual sensors and storing them in a desiccator. The anodic stripping currents in a 1 μM Cd^{2+} ion solution were recorded using new sensors after different storage times of up to 30 days. Figure 9a summarizes the sensor responses as a function of their respective storage times. In the figure, each point is the average of the readings taken on that respective day with three individual sensors. The results reveal that more than 90 % of the initial sensor response is maintained for the first 20 days, whereafter the response starts to decline. Such a long shelf life is highly advantageous for the practical application of the sensor, especially in remote areas.

The reusability of CPE-IIP was evaluated by recording the anodic stripping current of the same sensor 10 times in a row in a 1 μM Cd^{2+} ion solution. After each measurement, the CPE-IIP was leached with 0.1 M HNO_3 solution to ensure the complete removal of any adsorbed Cd species. Figure 9b shows the sensor responses as a function of the total number of measurements taken with the same sensor. In the figure, each point is the average of the readings from three different sensors tested in parallel. It is seen that the sensor response exhibits no significant change throughout the first four consecutive measurements, retaining more than 95 % of the initial response, before it deteriorates. This confirms the reusability of the sensor for a few measurements.

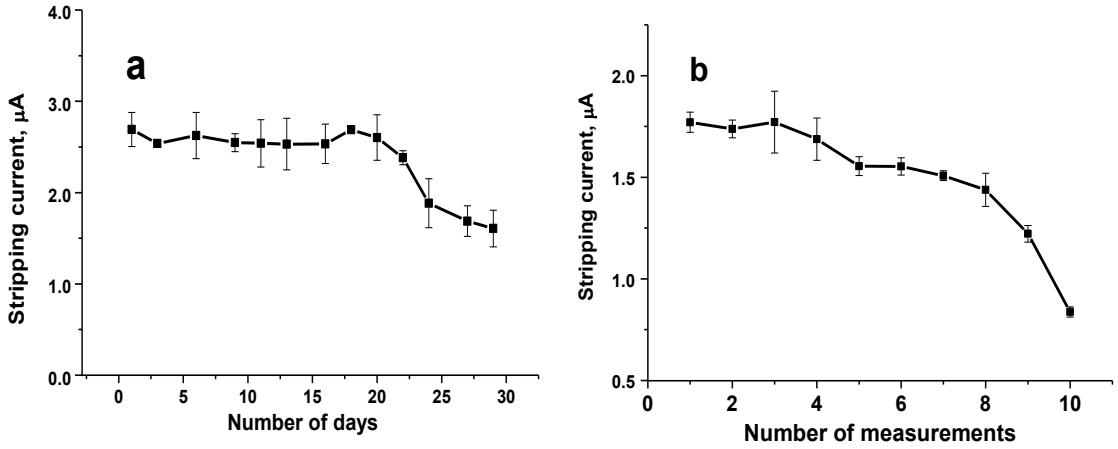

Figure 9. *(a) Reproducibility and (b) reusability of CPE-IIP*

Sensor studies summary

The CPE-IIP presented in this study has been designed in such a way that it benefits from the collective effects of the high electronic conductivity along the polyaniline backbone, which facilitates electrode design, the high surface area of the polymer's nanostructure, which enhances sensor sensitivity, and the specific binding ability of the chemically modified functional groups, which provides excellent sensitivity. In contrast to all other reports in the literature, it has also been shown that there is no significant cross-sensitivity to the most common anions. The results are compelling evidence of the superior performance of the IIP prepared in the present study for the given type of electrochemical sensor.

Conclusions

A sensitive and highly selective electrochemical sensor for Cd^{2+} ion detection in aqueous media was developed using ion-imprinting technology. The desired ion-imprinted polymer (IIP) was synthesized by copolymerizing anthranilic acid and 2-(1H-benzimidazol-2-yl) aniline in the presence of Cd^{2+} ions, followed by removing the Cd^{2+} ions through acid leaching. The IIP was used to modify a carbon paste electrode that was then tested for Cd^{2+} ion sensing using cyclic voltammetry and differential pulse anodic stripping voltammetry. Various electrode parameters, namely, Cd deposition potential, pH of deposition solution, deposition time, and active layer thickness, were optimized to achieve maximum performance. It was demonstrated that the sensor incorporating the IIP is applicable to the detection of Cd^{2+} ions in the concentration range from 1 to 10,000 nM with a LOD of 0.506 nM. The selectivity of the sensor was found to be promising even in the presence of 100 equivalents of many other ions. Shelf life and reusability were determined to be 20 days and 4 consecutive measurements, respectively. As the immediate next phase of development work, the present sensor, along with other sensors from our laboratory, is to be tested in real-world water samples collected in the industrial part of the Periyar river in Kerala State's Ernakulum District.

***Acknowledgements**: The authors acknowledge the Amrita Centre for Nanosciences and Molecular Medicine at Amrita Institute of Medical Sciences, Kochin, Kerala, for making available their scanning electron microscopy facilities for imaging studies, and St. Thomas College, Pala, Kerala, for making available their X-ray diffraction facilities and for support with the structural characterizations.*
AJ gratefully acknowledges the financial support obtained from SARD scheme of Kerala State Council for Science, Technology and Environment, Government of Kerala (002/SARD/2015/KSCSTE); EMR scheme of Science and Engineering Research Board, Government of India (EMR/2016/003755); SIRE scheme of Science and Engineering Research Board, Government of India (SIR/2022/000128); and Chief Minister's NavaKerala Postdoctoral Fellowship of Kerala State Higher Education Council (KSHEC-A3/344/Govt Kerala-NKPDF/2022). EV is grateful for a Fellowship awarded through the EMR scheme of Science and Engineering Research Board, Government of India (EMR/2016/003755).
CS gratefully acknowledges support from Gdańsk University of Technology by the DEC-7/1/ /2024/I.1a/No grant under the Nobelium 'Excellence Initiative - Research University' program.

***Conflict of interest**: The authors declare no conflict of interest.*

References

[1] G. Genchi, M. S. Sinicropi, G. Lauria, A. Carocci, A. Catalano, The effects of cadmium toxicity, *International Journal of Environmental Research and Public Health* **17** (2020) 3782. https://doi.org/10.3390/ijerph17113782
[2] Z. Khan, A. Elahi, D. A. Bukhari, A. Rehman, Cadmium sources, toxicity, resistance and removal by microorganisms – a potential strategy for cadmium eradication, *Journal of Saudi Chemical Society* **26** (2022) 101569. https://doi.org/10.1016/j.jscs.2022.101569
[3] P. Torres, A. Larrea Llopis, C. Sousa Melo, A. Rodrigues, Environmental impact of cadmium in a volcanic archipelago: research challenges related to a natural pollution source, *Journal of Marine Science and Engineering* **11** (2023) 100. https://doi.org/10.3390/jmse11010100
[4] A. Kubier, R. T. Wilkin, T. Pichler, Cadmium in soils and groundwater: a review, *Applied Geochemistry* **108** (2019) 104388. https://doi.org/10.1016/j.apgeochem.2019.104388
[5] V. R. Djordjevic, D. R. Wallace, A. Schweitzer, N. Boricic, D. Knezevic, S. Matic, N. Grubor, M. Kerkez, D. Radenkovic, Z. Bulat, B. Antonijevic, V. Matovic, A. Buha, Environmental cadmium exposure and pancreatic cancer: evidence from case control, animal and in vitro studies, *Environment International* **128** (2019) 353-361. https://doi.org/10.1016/j.envint.2019.04.048

[6] J. Tian, Z. Li, L. Wang, D. Qiu, X. Zhang, X. Xin, Z. Cai, B. Lei, Metabolic signatures for safety assessment of low-level cadmium exposure on human osteoblast-like cells, *Ecotoxicology and Environmental Safety* **207** (2021) 111257. https://doi.org/10.1016/j.ecoenv.2020.111257
[7] M. Si, J. Lang, The roles of metallothioneins in carcinogenesis, *Journal of Hematology & Oncology* **11** (2018) 107. https://doi.org/10.1186/s13045-018-0645-x
[8] S. Verma, P. Bhatt, A. Verma, H. Mudila, P. Prasher, E. R. Rene, Microbial technologies for heavy metal remediation: effect of process conditions and current practices, *Clean Technologies and Environmental Policy* **25** (2023) 1485-1507. https://doi.org/10.1007/s10098-021-02029-8
[9] A. A. Mohamed, A. Castagna, A. Ranieri, L. Sanità di Toppi, Cadmium tolerance in *Brassica juncea* roots and shoots is affected by antioxidant status and phytochelatin biosynthesis, *Plant Physiology and Biochemistry* **57** (2012) 15-22. https://doi.org/10.1016/j.plaphy.2012.05.002
[10] C. Baliardini, C.-L. Meyer, P. Salis, P. Saumitou-Laprade, N. Verbruggen, CATION EXCHANGER1 cosegregates with cadmium tolerance in the metal hyperaccumulator *Arabidopsis halleri* and plays a role in limiting oxidative stress in *Arabidopsis* Spp., *Plant Physiology* **169** (2015) 549-559. https://doi.org/10.1104/pp.15.01037
[11] S. He, X. Yang, Z. He, V. C. Baligar, Morphological and physiological responses of plants to cadmium toxicity: a review, *Pedosphere* **27** (2017) 421-438. https://doi.org/10.1016/S1002-0160(17)60339-4
[12] IARC Working Group on the Evaluation of Carcinogenic Risks to Humans, Beryllium, cadmium, mercury, and exposures in the glass manufacturing industry, *IARC Monographs on the Evaluation of Carcinogenic Risks to Humans*, Volume 58 (1993). https://www.ncbi.nlm.nih.gov/books/NBK499756/
[13] World Health Organization, Guidelines for drinking-water quality, Fourth edition incorporating the first and second addenda, Geneva, Switzerland (accessed 21 March 2025), https://www.who.int/publications/i/item/9789240045064
[14] I. Boevski, N. Daskalova, I. Havezov, Determination of barium, chromium, cadmium, manganese, lead and zinc in atmospheric particulate matter by inductively coupled plasma atomic emission spectrometry (ICP-AES), *Spectrochimica Acta Part B* **55** (2000) 1643-1657. https://doi.org/10.1016/S0584-8547(00)00265-2
[15] T. de A. Maranhão, E. Martendal, D. L. G. Borges, E. Carasek, B. Welz, A. J. Curtius, Cloud point extraction for the determination of lead and cadmium in urine by graphite furnace atomic absorption spectrometry with multivariate optimization using Box-Behnken design, *Spectrochimica Acta Part B* **62** (2007) 1019-1027. https://doi.org/10.1016/j.sab.2007.05.008
[16] G. Xiang, S. Wen, X. Wu, X. Jiang, L. He, Y. Liu, Selective cloud point extraction for the determination of cadmium in food samples by flame atomic absorption spectrometry, *Food Chemistry* **132** (2012) 532-536. https://doi.org/10.1016/j.foodchem.2011.10.053
[17] S. Jegadeesan, M. Dhamodaran, M. Azees, S. Shanmugapriya, Design and analysis of optical biosensor for detecting the heavy metals (cadmium) in the milk, *Sensor Letters* **16** (2018) 763-767, https://doi.org/10.1166/sl.2018.4018
[18] V. S. Pawar, S. D. Pawar, H. Mudila, A. D. Sheikh, A. Kaushik, Customization of an efficient and cost-effective optical biosensor for trace cadmium detection in milk samples, *Hybrid Advances* **8** (2025) 100367. https://doi.org/10.1016/j.hybadv.2024.100367
[19] K. Wu, S. Hu, J. Fei, W. Bai, Mercury-free simultaneous determination of cadmium and lead at a glassy carbon electrode modified with multi-wall carbon nanotubes, *Analytica Chimica Acta* **489** (2003) 215-221. https://doi.org/10.1016/S0003-2670(03)00718-9
[20] Nisha, Goverdhan, H. Mudila, A. Kumar, P. Prasher, A comprehensive review on material and techniques used for heavy metal detection in potable water, *AIP Conference Proceedings* **2800** (2023) 020186. https://doi.org/10.1063/5.0162879

[21] H. Mudila, P. Prasher, M. Kumar, H. Kapoor, A. Kumar, M. G. H. Zaidi, A. Verma, An insight into cadmium poisoning and its removal from aqueous sources by graphene adsorbents, *International Journal of Environmental Health Research* **29** (2019) 1-21. https://doi.org/10.1080/09603123.2018.1506568
[22] J. J. BelBruno, Molecularly imprinted polymers, *Chemical Reviews* **119** (2018) 94-119. https://doi.org/10.1021/acs.chemrev.8b00171
[23] O. S. Ahmad, T. S. Bedwell, C. Esen, A. Garcia-Cruz, S. A. Piletsky, Molecularly imprinted polymers in electrochemical and optical sensors, *Trends in Biotechnology* **37** (2019) 294-309. https://doi.org/10.1016/j.tibtech.2018.08.009
[24] P. M. S. Tchekwagep, R. D. Crapnell, C. E. Banks, K. Betlem, U. Rinner, F. Canfarotta, J. W. Lowdon, K. Eersels, B. van Grinsven, M. Peeters, J. McClements, A critical review on the use of molecular imprinting for trace heavy metal and micropollutant detection, *Chemosensors* **10** (2022) 296. https://doi.org/10.3390/chemosensors10080296
[25] S. Ramanavicius, A. Ramanavicius, Development of molecularly imprinted polymer based phase boundaries for sensors design (review), *Advances in Colloid and Interface Science* **305** (2022) 102693. https://doi.org/10.1016/j.cis.2022.102693
[26] S. Ramanavicius, U. Samukaite-Bubniene, V. Ratautaite, M. Bechelany, A. Ramanavicius, Electrochemical molecularly imprinted polymer based sensors for pharmaceutical and biomedical applications (review), *Journal of Pharmaceutical and Biomedical Analysis* **215** (2022) 114739. https://doi.org/10.1016/j.jpba.2022.114739
[27] M. Ghanei-Motlagh, M. A. Taher, Novel imprinted polymeric nanoparticles prepared by sol–gel technique for electrochemical detection of toxic cadmium(II) ions, *Chemical Engineering Journal* **327** (2017) 135-141. https://doi.org/10.1016/j.cej.2017.06.091
[28] L. Samandari, A. Bahrami, M. Shamsipur, L. Farzin, B. Hashemi, Electrochemical preconcentration of ultra-trace Cd^{2+} from environmental and biological samples prior to its determination using carbon paste electrode impregnated with ion imprinted polymer nanoparticles, *International Journal of Environmental Analytical Chemistry* **99** (2019) 172-186. https://doi.org/10.1080/03067319.2019.1583334
[29] T. Alizadeh, M. R. Ganjali, P. Nourozi, M. Zare, M. Hoseini, A carbon paste electrode impregnated with Cd^{2+} imprinted polymer as a new and high selective electrochemical sensor for determination of ultra-trace Cd^{2+} in water samples, *Journal of Electroanalytical Chemistry* **657** (2011) 98-106. https://doi.org/10.1016/j.jelechem.2011.03.029
[30] H. Ganjali, M. R. Ganjali, T. Alizadeh, F. Faridbod, P. Norouzi, Bio-mimetic cadmium ion imprinted polymer based potentiometric nano-composite sensor, *International Journal of Electrochemical Science* **6** (2011) 6085-6093. https://doi.org/10.1016/S1452-3981(23)19664-7
[31] Z. Dahaghin, P. A. Kilmartin, H. Z. Mousavi, Determination of cadmium(II) using a glassy carbon electrode modified with a Cd-ion imprinted polymer, *Journal of Electroanalytical Chemistry* **810** (2018) 185-190. https://doi.org/10.1016/j.jelechem.2018.01.014
[32] M. K. Lombello Coelho, H. Leijoto de Oliveira, F. Garcia De Almeida, K. Bastos Borges, C. R. Teixeira Tarley, A. C. Pereira, Development of carbon paste electrode modified with cadmium ion-imprinted polymer for selective voltammetric determination of Cd^{2+}, *International Journal of Environmental Analytical Chemistry* **97** (2018) 1378-1392. https://doi.org/10.1080/03067319.2018.1424330
[33] H. Ashkenani, M. A. Taher, Determination of cadmium(II) using carbon paste electrode modified with a Cd-ion imprinted polymer, *Microchimica Acta* **178** (2012) 53-60. https://doi.org/10.1007/s00604-012-0803-8
[34] S. A. Rezvani Ivari, A. Darroudi, M. H. Arbab Zavar, G. Zohuri, N. Ashraf, Ion imprinted polymer based potentiometric sensor for the trace determination of cadmium (II) ions, *Arabian Journal of Chemistry* **10** (2017) S864-S869. https://doi.org/10.1016/j.arabjc.2012.12.021

[35] A. Aravind, B. Mathew, Tailoring of nanostructured material as an electrochemical sensor and sorbent for toxic Cd(II) ions from various real samples, *Journal of Analytical Science and Technology* **9** (2018) 22. https://doi.org/10.1186/s40543-018-0153-1
[36] A. B. Abdallah, M. R. El-kholany, A. F. S. Molouk, T. A. Ali, A. A. El-Shafei, M. E. Khalifa, Selective and sensitive electrochemical sensors based on an ion imprinting polymer and graphene oxide for the detection of ultra-trace Cd(II) in biological samples, *RSC Advances* **11** 30771-30780 (2021). https://doi.org/10.1039/d1ra05489a
[37] W. Huang, Y. Liu, N. Wang, G. Song, X. Yin, L. Zhang, X. Ni, W. Xu, A sensitive electrochemical sensor based on ion imprinted polymers with gold nanoparticles for high selective detecting Cd (II) ions in real samples, *Journal of Inorganic and Organometallic Polymers and Materials* **31** (2021) 2043-2053. https://doi.org/10.1007/s10904-021-01892-8
[38] S. Hu, G. Gao, Y. Liu, J. Hu, Y. Song, X. Zou, An electrochemical sensor based on ion imprinted PPy/rGO composite for Cd(II) determination in water, *International Journal of Electrochemical Science* **14** (2019) 11714-11730. https://doi.org/10.20964/2019.11.56
[39] J. Wang, J. Hu, S. Hu, G. Gao, Y. Song, A novel electrochemical sensor based on electropolymerized ion imprinted PoPD/ERGO composite for trace Cd(II) determination in water, *Sensors* **20** (2020) 1004. https://doi.org/10.3390/s20041004
[40] L. Wang, J. Hu, W. Wei, S. Xiao, J. Wang, Y. Song, Y. Li, G. Gao, L. Qin, An electrochemical sensor based on three-dimensional porous reduced graphene and ion imprinted polymer for trace cadmium determination in water, *Sensors* **23** (2023) 9561. https://doi.org/10.3390/s23239561
[41] S. Wu, K. Li, X. Dai, Z. Zhang, F. Ding, S. Li, An ultrasensitive electrochemical platform based on imprinted chitosan/gold nanoparticles/graphene nanocomposite for sensing cadmium (II) ions, *Microchemical Journal* **155** (2020) 104710. https://doi.org/10.1016/j.microc.2020.104710
[42] J. Chen, Y. Chen, Y. Liang, Application of chitosan-N-doped graphene oxide ion-imprinted sensor in Cd (II) ions detection, *Diamond & Related Materials* **119** (2021) 108591. https://doi.org/10.1016/j.diamond.2021.108591
[43] Y. Zhang, Y. Liu, W. Xu, W. Huang, T. Chen, H. Ding, B. Wang, W. Yang, Novel electrochemical sensor based on rGO@TiO_2 composite material and ion-imprinted polymer modification for highly selective detection of cadmium ions in real samples, *Ionics* **30** (2024) 2345-2355. https://doi.org/10.1007/s11581-024-05410-x
[44] M. Costa, S. Di Masi, A. Garcia-Cruz, S. A. Piletsky, C. Malitesta, Disposable electrochemical sensor based on ion imprinted polymeric receptor for Cd(II) ion monitoring in waters, *Sensors and Actuators B* **383** (2023) 133559. https://doi.org/10.1016/j.snb.2023.133559
[45] J. Hu, M. Sedki, Y. Shen, A. Mulchandani, G. Gao, Chemiresistor sensor based on ion-imprinted polymer (IIP)-functionalized rGO for Cd(II) ions in water, *Sensors and Actuators B* **346** (2021) 130474. https://doi.org/10.1016/j.snb.2021.130474
[46] E. V. Varghese, B. Thomas, C. Schwandt, P. C. Ramamurthy, A. Joseph, Benzimidazole-modified polyaniline micro-shells for electrochemical detection of cadmium in aqueous solution, *Journal of Electrochemical Science and Engineering* **13** (2023) 275-286. http://dx.doi.org/10.5599/jese.1440
[47] J. Huang, S. Virji, B. H. Weiller, R. B. Kaner, Nanostructured polyaniline sensors, *Chemistry - A European Journal* **10** (2004) 1314-1319. https://doi.org/10.1002/chem.200305211
[48] K. Y. Presnyakov, P. S. Pidenko, S. A. Pidenko, I. R. Biryukov, N. A. Burmistrova, Molecularly imprinted polyaniline: synthesis, properties, application. A review, *Izvestiya of Saratov University. Chemistry. Biology. Ecology* **22** (2022) 142-149. https://doi.org/10.18500/1816-9775-2022-22-2-142-149

[49] H. Setiyanto, D. R. Purwaningsih, V. Saraswaty, N. Mufti, M. A. Zulfikar, Highly selective electrochemical sensing based on electropolymerized ion imprinted polyaniline (IIPANI) on a bismuth modified carbon paste electrode (CPE-Bi) for monitoring nickel(II) in river water, *RSC Advances* **12** (2022) 29554-29561. https://doi.org/10.1039/d2ra05196f
[50] F. Saadati, F. Ghahramani, H. Shayani-jam, F. Piri, M. R. Yaftian, Synthesis and characterization of nanostructure molecularly imprinted polyaniline/graphene oxide composite as highly selective electrochemical sensor for detection of *p*-nitrophenol, *Journal of the Taiwan Institute of Chemical Engineers* **86** (2018) 213-221. https://doi.org/10.1016/j.jtice.2018.02.019
[51] A. Drame, Š. Trafela, K. Žužek Rožman, Nanostructured molecularly imprinted polyaniline for acrylamide sensing, *Proceedings* **15** (2019) 37. https://doi.org/10.3390/proceedings2019015037
[52] J. Luo, J. Huang, Y. Wu, J. Sun, W. Wei, X. Liu, Synthesis of hydrophilic and conductive molecularly imprinted polyaniline particles for the sensitive and selective protein detection, *Biosensors and Bioelectronics* **94** (2017) 39-46. https://doi.org/10.1016/j.bios.2017.02.035
[53] Z. Chen, C. Wright, O. Dincel, T.-Y. Chi, J. Kameoka, A low-cost paper glucose sensor with molecularly imprinted polyaniline electrode, *Sensors* **20** (2020) 1098. https://doi.org/10.3390/s20041098
[54] P. Kumar, A. Joseph, P. C. Ramamurthy, S. Subramanian, Lead ion sensor with electrodes modified by imidazole-functionalized polyaniline, *Microchimica Acta* **177** (2012) 317-323. https://doi.org/10.1007/s00604-012-0787-4
[55] A. Joseph, P. C. Ramamurthy, S. Subramanian, Imidazole functionalized polyaniline: synthesis, characterization, and Cu (II) coordination studies, *Journal of Applied Polymer Science* **123** (2012) 526-534. https://doi.org/10.1002/app.34561
[56] E. T. Kang, K. G. Neoh, K. L. Tan, Polyaniline: a polymer with many interesting intrinsic redox states, *Progress in Polymer Science* **23** (1998) 277-324. https://doi.org/10.1016/S0079-6700(97)00030-0
[57] K. H. Wu, T. C. Chang, Y. T. Wang, Y. S. Hong, T. S. Wu, Interactions and mobility of copper(II)-imidazole-containing copolymers, *European Polymer Journal* **39** (2003) 239-245. https://doi.org/10.1016/S0014-3057(02)00229-X
[58] S. Patra, N. Munichandraiah, Insoluble poly(anthranilic acid) confined in Nafion membrane by chemical and electrochemical polymerization of anthranilic acid, *Synthetic Metals* **150** (2005) 285-290. https://doi.org/10.1016/j.synthmet.2005.03.001
[59] D. Giray, T. Balkan, B. Dietzel, A. Sezai Sarac, Electrochemical impedance study on nanofibers of poly(m-anthranilic acid)/polyacrylonitrile blends, *European Polymer Journal* **49** (2013) 2645-2653. https://doi.org/10.1016/j.eurpolymj.2013.06.012
[60] B. Butoi, A. Groza, P. Dinca, A. Balan, V. Barna, Morphological and structural analysis of polyaniline and poly(*o*-anisidine) layers generated in a DC glow discharge plasma by using an oblique angle electrode deposition configuration, *Polymers* **9** (2017) 732. https://doi.org/10.3390/polym9120732
[61] A. Mostafaei, A. Zolriasatein, Synthesis and characterization of conducting polyaniline nanocomposites containing ZnO nanorods, *Progress in Natural Science: Materials International* **22** (2012) 273-280. https://doi.org/10.1016/j.pnsc.2012.07.002
[62] M. Khalid, M. A. Tumelero, I. S. Brandt, V. C. Zoldan, J. J. S. Acuña, A. A. Pasa, Electrical conductivity studies of polyaniline nanotubes doped with different sulfonic acids, *Indian Journal of Materials Science* **2013** (2013) 718304. https://doi.org/10.1155/2013/718304
[63] J. P. Pouget, M. E. Józefowicz, A. J. Epstein, X. Tang, A. G. MacDiarmid, X-ray structure of polyaniline, *Macromolecules* **24** (1991) 779-789. https://doi.org/10.1021/ma00003a022

[64] B.-J. Kim, S.-G. Oh, M.-G. Han, S.-S. Im, Preparation of polyaniline nanoparticles in micellar solutions as polymerization medium, *Langmuir* **16** (2000) 5841-5841. https://doi.org/10.1021/la9915320
[65] P. Kumar, A. Joseph, P. C. Ramamurthy, S. Subramanian, Lead ion sensor with electrodes modified by imidazole-functionalized polyaniline, *Microchimica Acta* **177** (2012) 317-323. https://doi.org/10.1007/s00604-012-0787-4
[66] L.-L. Shen, G.-R. Zhang, W. Li, M. Biesalski, B. J. M. Etzold, Modifier-free microfluidic electrochemical sensor for heavy-metal detection, *ACS Omega* **2** (2017) 4593-4603. https://doi.org/10.1021/acsomega.7b00611